Effective velocity boundary condition at a mixed slip surface

M. Sbragaglia[1] and A.Prosperetti[1, 2]
[1]Department of Applied Physics, University of Twente,
P.O. Box 217, 7500 AE, Enschede, The Netherlands.
[2]Department of Mechanical Engineering, The Johns Hopkins University, Baltimore MD 21218, USA
(Dated: February 2, 2008)

This paper studies the nature of the effective velocity boundary conditions for liquid flow over a plane boundary on which small free-slip islands are randomly distributed. It is found that, to lowest order in the area fraction β covered by free-slip regions with characteristic size a, a macroscopic Navier-type slip condition emerges with a slip length of the order of $a\beta$. The study is motivated by recent experiments which suggest that gas nano-bubbles may form on solid walls and may be responsible for the appearance of a partial slip boundary conditions for liquid flow. The results are also relevant for ultra-hydrophobic surfaces exploiting the so-called "lotus effect".

PACS numbers: 47.15.-x,47.45.Gx,83.50.Lh,83.50.Rp

I. INTRODUCTION

The recent blossoming of research in micro-fluidics has prompted a renewed interest in the possibility of slip boundary conditions at the contact of a liquid with a solid wall [13, 14]. While many experiments have provided evidence for a violation of the classical no-slip boundary condition at small spatial scales [3, 5, 18, 28, 32, 33, 35, 36] the physical mechanisms responsible for this phenomenon are still unclear. An interesting possibility is the recent discovery of what appear to be small gas nano-bubbles or pockets attached to the wall [2, 6, 10, 11, 24, 27, 31]. The evidence for the existence of these nano-bubbles is somewhat indirect, but nevertheless compelling. It is also hypothesized and, sometimes, experimentally verified (see Watanabe et al. [33]), that gas pockets may form in cracks or other imperfections of the solid wall, thereby decreasing the overall wall stress.

In order to explore the macroscopic consequences of the existence of such drag-reducing gaseous structures on a solid wall, in this study we consider by statistical means the effective velocity boundary condition produced by a random distribution of small free-slip regions on an otherwise no-slip boundary. We consider both the three-dimensional problem, in which the regions are equal disks, and the two-dimensional problem, in which they are strips oriented perpendicularly to the flow. While idealized, these geometries provide some insight into the macroscopic effects of randomly distributed microscopic free-slip regions.

We find that, away from the wall, the velocity field appears to satisfy a partial-slip condition with a slip length proportional, to leading order, to the product of the length scale a of the free-slip islands and the area fraction β covered by them. After deriving a general result, we solve the problem to first order accuracy in β for both the two- and three- dimensional situations.

As discussed in section VII, our results are consistent with those of a recent paper by Lauga & Stone [14], who assumed a periodic distribution of free-slip patches on a boundary, as well as those of an older paper by Philip [17] who similarly investigated the effect of free-slip strips arranged periodically on a plane wall parallel or orthogonal to the direction of the flow.

The present results are also related to so-called "lotus effect" [1] exploited to obtain ultra-hydrophobic surfaces. Such surfaces are manufactured by covering a solid boundary with an array of hydrophobic micron-size posts which, due to the effect of surface tension, prevent a complete wetting of the wall [4, 15, 16]. In the space between the posts the liquid remains suspended away from the wall with its surface in contact only with the ambient gas and a concomitant reduction in the mean traction per unit area. Another instance of drag reduction by a similar mechanism has also been reported in Watanabe et al. [33]. These authors studied the pressure drop in the flow of a viscous liquid in a tube the wall of which contained many fine grooves which prevented a complete wetting of the boundary.

The approach used in this paper is mainly suggested by the theory of multiple scattering [8, 29, 30] and was used before to derive the effective boundary conditions at a rough surface for the Laplace and Stokes problems [22, 23]

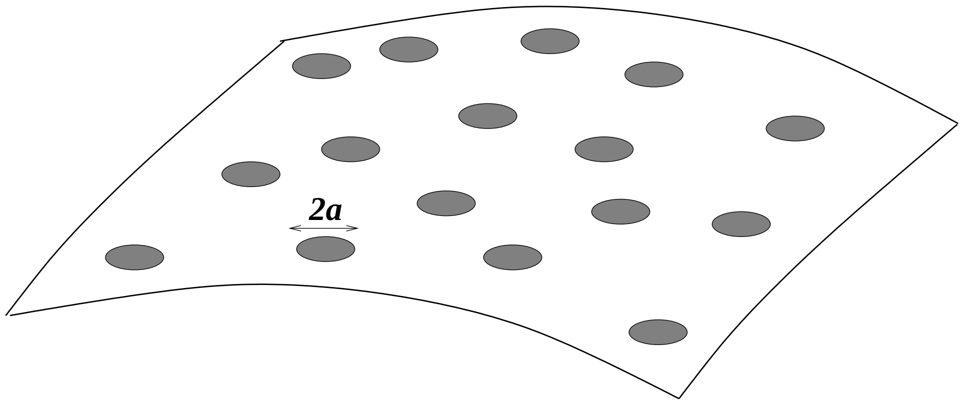

FIG. 1: Solid no-slip boundary with a random distribution of equal circular free-slip areas.

II. FORMULATION

We consider the flow in the neighborhood of a locally plane boundary [37] $\mathcal{B}$ with a composite micro-structure which dictates free-slip conditions on certain areas s^1, $s^2, \ldots, s^N$ and no-slip conditions on the remainder $\mathcal{B} - \cup_{\alpha=1}^N s^\alpha$ (figure 1). If each "island" s^α is sufficiently small, and $\cup_{\alpha=1}^N s^\alpha$ is also sufficiently small (both in a sense to be made precise later), near the boundary the flow is described by the Stokes equations:

$$\boldsymbol{\nabla} p = \mu \nabla^2 \boldsymbol{u}\,, \qquad \boldsymbol{\nabla}\cdot\boldsymbol{u} = 0\,, \tag{1}$$

in which p and $\boldsymbol{u}$ are the pressure and velocity fields and μ the viscosity. On the free-slip regions $\boldsymbol{u}$ satisfies the condition of vanishing tangential stress:

$$\boldsymbol{t}_J \cdot (\boldsymbol{\tau}\cdot\hat{\boldsymbol{n}}) = 0 \qquad \boldsymbol{x} \in s^\alpha \qquad \alpha = 1,\, 2,\, \ldots,\, N \qquad J = 2,\, 3 \tag{2}$$

where $\boldsymbol{t}_2$ and $\boldsymbol{t}_3$ are two unit vectors in the plane and $\boldsymbol{\tau}$ the viscous stress tensor, while, on the rest of the surface,

$$\boldsymbol{u} = 0 \qquad \boldsymbol{x} \notin \cup_{\alpha=1}^N s^\alpha\,. \tag{3}$$

The normal velocity vanishes everywhere on $\mathcal{B}$.

We start by decomposing the solution $(p,\, \boldsymbol{u})$ as

$$\boldsymbol{u} = \boldsymbol{u}^0 + \sum_{\alpha=1}^N \boldsymbol{v}^\alpha\,, \qquad p = p^0 + \sum_{\alpha=1}^N q^\alpha \tag{4}$$

Here $\boldsymbol{u}^0$ and p^0 are the (deterministic) solution satisfying the usual no slip condition on the entire boundary $\mathcal{B}$ while the fields $(q^\alpha, \boldsymbol{v}^\alpha)$ account for the effect of the α-th island. We define these local fields so that $\boldsymbol{v}^\alpha$ vanishes everywhere on $\mathcal{B}$ except on s^α, where it is such that the free-slip condition (2) is satisfied. To express this condition it is convenient to define

$$\boldsymbol{w}^\alpha = \boldsymbol{u}^0 + \sum_{\beta\neq\alpha} \boldsymbol{v}^\beta\,, \qquad r^\alpha = p^0 + \sum_{\beta\neq\alpha} q^\beta\,, \tag{5}$$

so that, for every $\alpha = 1,\, 2,\, \ldots,\, N$,

$$\boldsymbol{u} = \boldsymbol{v}^\alpha + \boldsymbol{w}^\alpha\,, \qquad p = q^\alpha + r^\alpha\,. \tag{6}$$

On s^α, then, $\boldsymbol{v}^\alpha$ satisfies

$$\boldsymbol{t}_J \cdot (\boldsymbol{\tau}^{v\alpha}\cdot\hat{\boldsymbol{n}}) = -\,\boldsymbol{t}_J \cdot (\boldsymbol{\tau}^{w\alpha}\cdot\hat{\boldsymbol{n}}) \qquad \boldsymbol{x} \in s^\alpha \qquad J = 2, 3 \tag{7}$$

where

$$\boldsymbol{\tau}^{v\alpha} = \mu\left[\boldsymbol{\nabla}\boldsymbol{v}^\alpha + (\boldsymbol{\nabla}\boldsymbol{v}^\alpha)^T\right], \qquad \tau^{w\alpha} = \mu\left[\boldsymbol{\nabla}\boldsymbol{w}^\alpha + (\boldsymbol{\nabla}\boldsymbol{w}^\alpha)^T\right], \tag{8}$$

the superscript T denoting the transpose. Clearly

$$\boldsymbol{v}^\alpha \to 0, \qquad q^\alpha \to 0 \qquad \text{as} \qquad |\boldsymbol{x} - \boldsymbol{y}^\alpha| \to \infty \tag{9}$$

with $\boldsymbol{y}^\alpha$ a reference point on the α-th island. It is evident that both fields $\boldsymbol{v}^\alpha$ and $\boldsymbol{w}^\alpha$ satisfy the Stokes equations. In the terminology of multiple scattering, they are often referred to as the 'scattered' and 'incident' fields, respectively [8, 21].

III. AVERAGING

We assume that the free-slip islands are identical circular disks with radius a, centered at $\boldsymbol{y}^\alpha$, with $\alpha = 1, 2, \ldots, N$. We make use of the method of ensemble averaging and consider an ensemble of surfaces differing from each other only in the arrangement of the N free-slip islands. Each arrangement, or configuration, is denoted by $\mathcal{C}^N = (\boldsymbol{y}^1, \boldsymbol{y}^2, ..., \boldsymbol{y}^N)$. A particular configuration will then occur with a probability $P(\mathcal{C}^N) = P(N)$ normalized according to:

$$\frac{1}{N!}\int d^2y^1 \ldots \int d^2y^N P(\boldsymbol{y}^1, \ldots, \boldsymbol{y}^N) \equiv \frac{1}{N!}\int d\mathcal{C}^N P(N) = 1. \tag{10}$$

The ensemble-average velocity is defined as

$$\langle \boldsymbol{u}\rangle(\boldsymbol{x}) = \frac{1}{N!}\int \mathrm{d}\mathcal{C}^N P(N)\, \boldsymbol{u}(\boldsymbol{x}|N) \tag{11}$$

where the notation $\boldsymbol{u}(\boldsymbol{x}|N)$ stresses the dependence of the exact field not only on the point $\boldsymbol{x}$, but also on the configuration of the N islands. In view of the fact that $\boldsymbol{u}^0$ is independent of the configuration of the disks, substitution of the decomposition (4) into (11) gives

$$\langle \boldsymbol{u}\rangle(\boldsymbol{x}) = \boldsymbol{u}^0(\boldsymbol{x}) + \frac{1}{N!}\sum_{\alpha=1}^{N}\int \mathrm{d}\mathcal{C}^N P(N)\, \boldsymbol{v}^\alpha(\boldsymbol{x}|N). \tag{12}$$

Since the disks are identical, each one gives the same contribution to the integral. Upon introducing the conditional probability $P(N-1|\boldsymbol{y}^1)$ defined so that $P(N) = P(\boldsymbol{y}^1)\, P(N-1|\boldsymbol{y}^1)$, we may therefore write

$$\langle \boldsymbol{u}\rangle(\boldsymbol{x}) = \boldsymbol{u}^0(\boldsymbol{x}) + \frac{1}{(N-1)!}\int \mathrm{d}\mathcal{C}^N P(\boldsymbol{y}^1)\, P(N-1|\boldsymbol{y}^1)\, \boldsymbol{v}^1(\boldsymbol{x}|\boldsymbol{y}^1, N-1) \tag{13}$$

or, in terms of the conditional average

$$\langle \boldsymbol{v}^1\rangle_1(\boldsymbol{x}|\boldsymbol{y}^1) = \frac{1}{(N-1)!}\int \mathrm{d}\mathcal{C}^{N-1} P(N-1|\boldsymbol{y}^1)\, \boldsymbol{v}^1(\boldsymbol{x}|\boldsymbol{y}^1, N-1), \tag{14}$$

$$\langle \boldsymbol{u}\rangle(\boldsymbol{x}) = \boldsymbol{u}^0(\boldsymbol{x}) + \int_{\mathcal{B}} d^2y\, P(\boldsymbol{y})\, \langle \boldsymbol{v}\rangle_1(\boldsymbol{x}|\boldsymbol{y}) \tag{15}$$

where the integral is over the entire boundary. For convenience, here and in the following, we drop the superscript 1 on the quantities referring to disc 1. Since $\boldsymbol{v}^\alpha$ and q^α satisfy the Stokes equations everywhere, so do $\langle \boldsymbol{v}\rangle_1$ and $\langle q\rangle_1$. The boundary conditions are

$$\langle \boldsymbol{v}\rangle_1 = 0 \qquad \boldsymbol{x} \notin s \tag{16}$$

while

$$\boldsymbol{t}_J \cdot (\langle \boldsymbol{\tau}^v\rangle_1 \cdot \hat{\boldsymbol{n}}) = -\boldsymbol{t}_J \cdot (\langle \boldsymbol{\tau}^w\rangle_1 \cdot \hat{\boldsymbol{n}}) \qquad \boldsymbol{x} \in s \qquad J = 2, 3. \tag{17}$$

Note that

$$\langle \tau^w_{jk} \rangle_1 \;=\; \mu \left(\langle \partial_j w_k \rangle_1 + \langle \partial_k w_j \rangle_1 \right) \;=\; \mu \left(\partial_j \langle w_k \rangle_1 + \partial_k \langle w_j \rangle_1 \right) \,, \tag{18}$$

and similarly for $\langle \tau^v_{jk} \rangle_1$ since averaging and differentiation commute as is evident from the definition (11). The normal velocity vanishes everywhere:

$$\langle v_\perp \rangle_1 \;\equiv\; \hat{\boldsymbol{n}} \cdot \langle \boldsymbol{v} \rangle_1 \;=\; 0 \qquad \boldsymbol{x} \in \mathcal{B} \,. \tag{19}$$

It may be noted that $P(\boldsymbol{x})$ is just the number density of free-slip islands per unit surface area of the boundary; the area fraction β covered by these islands is

$$\beta(\boldsymbol{x}) \;=\; \int_{|\boldsymbol{x}-\boldsymbol{y}|\le a} P(\boldsymbol{y})\, d^2 y \;\simeq\; \pi a^2 P(\boldsymbol{x}) + O(a^2/L^2) \tag{20}$$

where L, assumed much greater than a, is the characteristic length scale for variations of the number density.

The framework just described can be readily extended to disks of unequal radius, and to non-isotropic islands such as ellipses. In both cases the probability density would depend on a suitably enlarged list of variables such as the disk radius, the characteristic size, orientation and aspect ratio of the ellipses, and so on.

IV. THE EFFECTIVE BOUNDARY CONDITION

Now we derive a formal expression for the effective boundary condition on $\mathcal{B}$. To this end, let $G^W_{ij}(\boldsymbol{y};\boldsymbol{x})$ be the Green's tensor for the Stokes problem vanishing at infinity and on the plane boundary $\mathcal{B}$. Then

$$\langle v_j \rangle_1(\boldsymbol{x}|\boldsymbol{y}) \;=\; \int_{\mathcal{B}} \left[\langle -q\hat{n}_i + (\boldsymbol{\tau}^v \cdot \hat{\boldsymbol{n}})_i \rangle_1(\boldsymbol{s}|\boldsymbol{y})\, G^W_{ij}(\boldsymbol{s};\boldsymbol{x}) + \langle v_j \rangle_1(\boldsymbol{z}|\boldsymbol{y})\, T^W_{ijk}(\boldsymbol{s};\boldsymbol{x}) n_k \right] d^2 s \tag{21}$$

where T^W_{ijk} is the stress Green's function associated to G^W_{ij} and the integral is extended over the entire plane boundary [12, 19] This formula can be considerably simplified recalling that, on the boundary, $\boldsymbol{v}$ vanishes everywhere outside s while G^W vanishes everywhere. Furthermore, on s, the tangential tractions also vanish. Hence, upon taking the x_1-axis along the normal with $x_1 = 0$ on the plane, we have

$$\langle v_j \rangle_1(\boldsymbol{x}|\boldsymbol{y}) \;=\; \int_s \langle v_j \rangle_1(\boldsymbol{s}|\boldsymbol{y})\, T^W_{ij1}(\boldsymbol{s};\boldsymbol{x})\, d^2 s \tag{22}$$

where now the integration is extended only over the free-slip island. We now consider points $\boldsymbol{x}$ such that $|\boldsymbol{x}-\boldsymbol{s}| \gg a$, but such that $|\boldsymbol{x}-\boldsymbol{s}|$ is sufficiently small to be in the Stokes region adjacent to the boundary. It can be verified that, in this range, we have

$$T^W_{ij1}(\boldsymbol{s};\boldsymbol{x}) \;=\; 2T_{ij1}(\boldsymbol{y};\boldsymbol{x}) \left[1 + O\left(\frac{a}{|\boldsymbol{x}-\boldsymbol{s}|} \right) \right] \tag{23}$$

where T_{ijk} is the free-space stress Green's function:

$$T_{ijk}(\boldsymbol{y};\boldsymbol{x}) \;=\; \frac{3}{4\pi} \frac{(y_i - x_i)(y_j - x_j)(y_k - x_k)}{|\boldsymbol{y}-\boldsymbol{x}|^5} \,. \tag{24}$$

Thus, (22) becomes

$$\langle v_j \rangle_1(\boldsymbol{x}|\boldsymbol{y}) \;\simeq\; 2\pi a^2 T_{ij1}(\boldsymbol{y};\boldsymbol{x}) V_i(\boldsymbol{y}) \tag{25}$$

where

$$V_i(\boldsymbol{y}) \;=\; \frac{1}{\pi a^2} \int_{|\boldsymbol{s}-\boldsymbol{y}|\le a} \langle v_i \rangle_1(\boldsymbol{s}|\boldsymbol{y})\, d^2 s \tag{26}$$

is the average velocity over the disk centered at $\boldsymbol{y}$. Note that $V_1 = 0$ as $v_1 = 0$. This result may now be inserted into the expression (15) for the average field to find

$$\langle u_j \rangle(\boldsymbol{x}) \;=\; u_j^0(\boldsymbol{x}) + 2\pi a^2 \int d^2y\, P(\boldsymbol{y})\, T_{ij1}(\boldsymbol{y};\boldsymbol{x}) V_i(\boldsymbol{y})\,. \tag{27}$$

We now take the 'inner limit' of (27) by letting the field point $\boldsymbol{x}$ approach $\mathcal{B}$ to find (see e.g. Pozrikidis [19] pp. 23 and 27)

$$\lim_{x_1 \to 0} T_{ij1}(\boldsymbol{y};\boldsymbol{x}) \;=\; \frac{1}{2}\delta_{ij}\delta(\boldsymbol{x}-\boldsymbol{y}) \tag{28}$$

so that

$$\langle \boldsymbol{u}_\parallel \rangle(\boldsymbol{x}) \;=\; \pi a^2 P(\boldsymbol{x})\, \boldsymbol{V}(\boldsymbol{x}) \tag{29}$$

where $\boldsymbol{u}_\parallel$ is the velocity component parallel to the boundary. Since the problem is linear, a dimensionless tensor W_{ij} must exist such that

$$V_i \;=\; \frac{a}{\mu} W_{ij} \left(\langle \boldsymbol{\tau}^w \rangle_1 \cdot \hat{\boldsymbol{n}} \right)_j \tag{30}$$

so that the average field satisfies the partial slip condition

$$\langle \boldsymbol{u}_\parallel \rangle(\boldsymbol{x}) \;=\; \frac{\pi a^3}{\mu} P(\boldsymbol{x})\, \mathsf{W} \cdot \left(\langle \boldsymbol{\tau}^w \rangle_1 \cdot \hat{\boldsymbol{n}} \right) \;\simeq\; \frac{a\beta}{\mu}\, \mathsf{W} \cdot \left(\langle \boldsymbol{\tau}^w \rangle_1 \cdot \hat{\boldsymbol{n}} \right)\,. \tag{31}$$

This equation shows that the slip length is of the order of $a\beta$.

We can now be more specific about the assumption made at the beginning of section II as to the validity of the Stokes equations near the wall. The condition for this assumption is evidently that the Reynolds number

$$Re \;=\; \frac{2a|\boldsymbol{V}|}{\nu} \tag{32}$$

with ν the kinematic viscosity, be sufficiently small. Equation (30) shows that $|\boldsymbol{V}|$ is of the order of a/μ times the magnitude of the wall shear stress; a precise result in a particular case is derived in Appendix A.

V. FIRST-ORDER PROBLEM

While exact, the result (31) expresses the effective boundary condition on the unconditionally averaged field $\langle \boldsymbol{u} \rangle$ in terms of the conditionally averaged wall stress $\langle \boldsymbol{\tau}^w \rangle_1$. In order to obtain the conditionally averaged velocity $\langle \boldsymbol{u} \rangle_1$ necessary to evaluate this quantity, one would need an effective boundary condition which would involve the wall stress averaged conditionally with the position of two free-slip islands prescribed, and so on. This is the well-known closure problem that arises in ensemble averaging. An explicit solution can only be found by truncating somehow the resulting hierarchy of equations.

The lowest-order non-trivial truncation can be effected with an accuracy of first order in the area fraction β. It is well known that, in this limit, the average 'incident' $\langle \boldsymbol{w} \rangle$ may be approximated by the unconditional average $\langle \boldsymbol{u} \rangle$ so that

$$\langle \boldsymbol{u}_\parallel \rangle(\boldsymbol{x}) \;=\; \frac{a\beta}{\mu}\, \mathsf{W} \cdot \left[\langle \boldsymbol{\tau} \rangle(\boldsymbol{x}) \cdot \hat{\boldsymbol{n}} \right] + o(\beta)\,. \tag{33}$$

If the density of the islands is small, since $\boldsymbol{w}$ accounts for the effect of all the other islands on the one centered at $\boldsymbol{y}$, $\langle \boldsymbol{w} \rangle_1$ is slowly varying near $\boldsymbol{y}$ so that

$$\langle \boldsymbol{w} \rangle_1(\boldsymbol{x}) \;=\; \langle \boldsymbol{w} \rangle_1(\boldsymbol{y}) + \left[(\boldsymbol{x}-\boldsymbol{y}) \cdot \boldsymbol{\nabla} \right] \langle \boldsymbol{w} \rangle_1(\boldsymbol{y}) + \ldots \tag{34}$$

and, therefore,

$$\langle \tau_{jk}^w \rangle_1 \;=\; \mu \left(\partial_j \langle w_k \rangle_1 + \partial_k \langle w_j \rangle_1 \right) \;\simeq\; \mu \left(\partial_j \langle u_k \rangle + \partial_k \langle u_j \rangle \right) \;=\; \langle \tau_{jk} \rangle \tag{35}$$

is approximately constant over the island $|\boldsymbol{x}-\boldsymbol{y}| \leq a$. The velocity field $\langle \boldsymbol{v}\rangle_1$ is therefore the solution of the Stokes equations (1) vanishing at infinity and whose normal component vanishes on the entire plane; the two tangential components vanish for $|\boldsymbol{x}-\boldsymbol{y}| > a$ while, for $J = 2, 3$ and $|\boldsymbol{x}-\boldsymbol{y}| < a$

$$\boldsymbol{t}_J \cdot \left(\left[\boldsymbol{\nabla}\langle \boldsymbol{v}\rangle_1 + (\boldsymbol{\nabla}\langle \boldsymbol{v}\rangle_1)^T\right] \cdot \hat{\boldsymbol{n}}\right) \;=\; -\frac{1}{\mu}\boldsymbol{t}_J \cdot (\langle \boldsymbol{\tau}\rangle \cdot \hat{\boldsymbol{n}}) \;= \text{const.} \tag{36}$$

This problem is solved in the Appendix A where it is shown that

$$W_{ij} \;=\; \frac{8}{9\pi}\delta_{ij} \tag{37}$$

so that the effective boundary condition (31) becomes

$$\langle \boldsymbol{u}_{\|}\rangle(\boldsymbol{x}) \;=\; \frac{8}{9\pi}\frac{a}{\mu}\beta(\boldsymbol{x})(\langle \boldsymbol{\tau}\rangle(\boldsymbol{x}) \cdot \hat{\boldsymbol{n}}) + o(\beta)\,. \tag{38}$$

It may be expected that, if the islands had an intrinsic direction (e.g., an elliptical shape) and were not randomly oriented, the tensor W_{ij} would not be isotropic so that the average surface traction and surface velocity would not be collinear.

VI. THE TWO-DIMENSIONAL CASE

The previous analysis can also be applied to the analogous two-dimensional case, i.e. a surface with a random distribution of parallel, or nearly parallel, free-shear strips of width a oriented perpendicular to the flow direction. The developments at the beginning of section IV are still valid and we may start from (22) noting that, in place of (24), we have

$$T_{ijk}(\boldsymbol{y};\boldsymbol{x}) \;=\; \frac{1}{\pi}\frac{(y_i - x_i)(y_j - x_j)(y_k - x_k)}{|\boldsymbol{y}-\boldsymbol{x}|^4}\,. \tag{39}$$

so that (22) becomes, in this case,

$$\langle v_j\rangle_1(\boldsymbol{x}|\xi) \;\simeq\; 2aT_{j21}(\xi;\boldsymbol{x})V_2(\xi)\,, \tag{40}$$

where ξ is the coordinate in the direction parallel to the plane. Here

$$V_2(\xi) \;=\; \frac{1}{a}\int_{|\zeta-\xi|\leq a} \langle v_2\rangle_1(\zeta|\xi)\, d\zeta \tag{41}$$

is again the average velocity over the strip centered at ξ. The expression (15) for the average field is modified to

$$\langle u_j\rangle(\boldsymbol{x}) \;=\; u_{0j}(\boldsymbol{x}) + 2a\int d\xi\, P(\xi)\, T_{j21}(\xi;\boldsymbol{x})V_2(\xi)\,. \tag{42}$$

The analog of (28) is still valid so that

$$\langle u_2\rangle(\xi) \;=\; a\,P(\xi)\,V_2(\xi) \tag{43}$$

where u_2 is the velocity component parallel to the boundary.

As before, from the linearity of the problem we deduce the existence of a dimensionless quantity W such that

$$V \;=\; \frac{a}{\mu}W\langle \tau^w_{xy}\rangle_1 \tag{44}$$

so that the average field satisfies the partial slip condition

$$\langle u\rangle(\xi) \;=\; \frac{a}{\mu}\beta(\xi)\,W\langle \tau^w_{xy}\rangle_1 \tag{45}$$

where we have used the fact that the fraction of the boundary covered by the free-slip strips is now given by

$$\beta(\xi) = \int_{|\zeta-\xi|\leq a} P(\zeta)\, d\zeta \simeq aP(\xi) + O(a^2/L^2)\,. \tag{46}$$

The solution of the problem in the dilute limit is given in Appendix B. One find

$$W = \frac{\pi}{16} \tag{47}$$

so that the effective boundary condition becomes

$$\langle u\rangle(\xi) = \frac{\pi}{16}\frac{a}{\mu}\beta(\xi)\langle\tau_{xy}\rangle + o(\beta) \tag{48}$$

VII. CONCLUSIONS

We have derived an effective velocity boundary condition on a wall covered by a random arrangement of free-slip disks or two-dimensional strips. For the case of disks we have found that, to leading order in the fraction β of the unit area covered by the disks, the velocity satisfies a Navier partial slip condition with a slip length ℓ given by

$$\ell = \frac{8}{9\pi}\beta\, a \tag{49}$$

where a is the common radius of the disks.

One of the motivations of this study was the possibility that gaseous structures attached to the solid wall, such as nano-bubbles, could furnish a mechanism explaining the partial slip observed by several investigators and it is therefore interesting to examine how the result (49) compares with available data. A full comparison would require simultaneous data for ℓ, β and a. The only paper in which all this information is available seems to be the study by Watanabe et al. [33], whose data, according to Lauga & Stone [14] imply a slip length of about 450 μm and an area fraction $\beta \simeq 10\%$. With these data, (49) gives $a \simeq 13$ μm. Rather than disks as in the present study, the free-slip islands in Watanabe et al.'s work were cracks with a width of about 10 μm and a length of the order 100 μm. If an equivalent radius is estimated as $\pi a^2 = 10 \times 100$ μm^2, one finds $a \simeq 18$ μm which is not too far from the estimate obtained from (49).

The study of Simonsen et al. [24] quotes $a \simeq 75$ nm and $\beta \simeq 60\%$. With these values, the estimate (49) gives $\ell \simeq 13$ nm. Although, for such large β's, the relation is probably not very accurate, this value for the slip length is in the ballpark measured by several investigators, such as Zhu & Granick [36], who report $0 \leq \ell < 40$ nm for water, and Craig et al. [5], who report $0 \leq \ell < 18$ nm, for water-sucrose solutions.

Wu, Zhang, Zhang, Li, Sun, Zhang, Li & Hu [34] measure a very low nano-bubble number density of about 3 bubbles per 10 μm^2, with typical radii of the order of 100 nm, which gives $\beta \simeq 1\%$ and $\ell \simeq 0.3$ nm. This is small, but not out of line with some of the existing measurements.

The radius of surface nano-bubbles reported by Holmberg et al. [10] is in the range 25 to 65 nm while that reported by Ishida et al. [11] is of the order of 300 nm. With an area coverage of 20%, we can estimate a slip length between about 2 and 20 nm. Again, these numerical values are in the expected range.

Tyrrell & Attard [31] and Steitz et al. [27] measure an area coverage of the order of 90%, which falls well outside the domain of applicability of our result. Unfortunately, neither group measured the slip length.

Tretheway & Meinhart [28] measured a slip length of about 1 μm, but made no estimates of area coverage or bubble size. With $\ell = 1$ μm, (49) gives a bubble radius a as large as 3.5 μm even for $\beta \sim 1$, and larger still for smaller β. This is another case for which it would be of great interest to have some information on the surface structures.

It is also of interest to compare our results with those of Lauga & Stone [14] obtained for flows in a tube with a periodic arrangement of free-slip rings perpendicular to the flow. For large tube radius, this arrangement should be comparable to our two-dimensional analysis. Their solution

is numerical, but they provide an approximate analytic expressions valid for large tube radius, namely

$$\ell = \frac{H}{2\pi} \log\left(\sec\left(\frac{\pi}{2}\beta\right)\right) \tag{50}$$

where H is the spatial period. Upon expanding for small β, we find

$$\ell \simeq \frac{\pi}{16} H\beta^2 \tag{51}$$

which, with the identification $H\beta = a$, is in precise agreement with our two-dimensional result (48). Lauga & Stone also give a similar result for free-slip strips parallel to the flow, but this situation is not comparable with either one of the two that we have considered.

Acknowledgments

We are indebted with Dr. S.M. Dammer for directing us to many pertinent references. M.S. is grateful to Prof. D. Lohse for several enlightening discussions and to STW (Nanoned programme) for financial support.

APPENDIX A: SOLUTION OF THE THREE-DIMENSIONAL PROBLEM

We take the center of the island as the origin, with the z-axis normal to the plane and the x-axis parallel to the tangential component of the traction $\langle \boldsymbol{\tau} \rangle \cdot \boldsymbol{n}$. Since the normal velocity component vanishes, with this choice of coordinates we require

$$\frac{\partial v_x}{\partial z} = S\,, \qquad \frac{\partial v_y}{\partial z} = 0\,, \tag{A1}$$

where

$$S = -\frac{1}{\mu}\left(\langle \boldsymbol{\tau} \rangle \cdot \boldsymbol{n}\right)_x . \tag{A2}$$

Here and in the following we write $\boldsymbol{v}$ in place of $\langle \boldsymbol{v} \rangle_1$ for convenience. Furthermore we measure lengths with respect to the island radius a, although no special notation will be used to indicate dimensionless variables. It is convenient to adopt a system of cylindrical coordinates (r, θ, z) in which $v_x = v_r \cos\theta - v_\theta \sin\theta$, $v_y = v_r \sin\theta + v_\theta \cos\theta$, in terms of which the condition (**??**) becomes, after suitable non-dimensionalization,

$$\frac{\partial v_r}{\partial z} = S\cos\theta\,, \qquad \frac{\partial v_\theta}{\partial z} = -S\sin\theta\,. \tag{A3}$$

Following Ranger [20] (see also [7, 25]), we represent the velocity field in the form

$$\boldsymbol{v} = \boldsymbol{\nabla} \times \left[\frac{\sin\theta}{r}\chi(r,z)\hat{\boldsymbol{e}}_z + \boldsymbol{\nabla} \times \left(\frac{\cos\theta}{r}\psi(r,z)\hat{\boldsymbol{e}}_z\right)\right] \tag{A4}$$

where $\hat{\boldsymbol{e}}_z$ is a unit vector normal to the plane and

$$\mathsf{L}\chi = 0 \qquad \mathsf{L}^2\psi = 0 \tag{A5}$$

with

$$\mathsf{L} = \frac{\partial^2}{\partial r^2} - \frac{1}{r}\frac{\partial}{\partial r} + \frac{\partial^2}{\partial z^2}. \tag{A6}$$

The Cartesian velocity components follow from (A4) as

$$v_x(r,z,\theta) = \frac{1}{2} r\partial_r \left[\frac{1}{r^2}\left(\partial_z\psi - \chi\right)\right] \cos 2\theta + \frac{1}{2r}\partial_r\left(\partial_z\psi + \chi\right) \tag{A7}$$

$$v_y(r,z,\theta) = \frac{1}{2} r \partial_r \left[\frac{1}{r^2} \left(\partial_z \psi - \chi \right) \right] \sin 2\theta \tag{A8}$$

$$v_z(r,z,\theta) = -\partial_r \left(\frac{1}{r} \partial_r \psi \right) \cos\theta \tag{A9}$$

while, from the Stokes equation, the pressure is found as

$$p(r,z,\theta) \;=\; \mu \frac{\cos\theta}{r} \frac{\partial}{\partial z} \mathsf{L}\psi\,. \tag{A10}$$

The solution of (A5) is sought in the form of Hankel transforms with the result

$$\psi \;=\; rz \int_0^\infty e^{-kz} J_1(kr)\, \tilde{\psi}(k)\, dk \tag{A11}$$

$$\chi \;=\; r \int_0^\infty e^{-kz} J_1(kr)\, \tilde{\chi}(k)\, dk\,. \tag{A12}$$

The functions $\tilde{\psi}$ and $\tilde{\chi}$ must be determined by imposing the boundary conditions. Upon substituting (A11) and (A12) into (A7) and (A8), we find that the no-slip condition outside the disk is satisfied provided that

$$\int_0^\infty J_1(kr)\left(\psi(k) + \chi(k)\right) dk = \frac{d}{r} \qquad r > 1 \tag{A13}$$

$$\int_0^\infty J_1(kr)\left(\psi(k) - \chi(k)\right) dk = 0 \qquad r > 1 \tag{A14}$$

where d is an integration constant to be determined later. The stress condition (A1) inside the disk is satisfied provided that

$$\int_0^\infty J_1(kr)\left(-2\psi(k) - \chi(k)\right) k\ dk = Sr \qquad 0 < r < 1 \tag{A15}$$

$$\int_0^\infty J_1(kr)\left(-2\psi(k) + \chi(k)\right) k\ dk = br \qquad 0 < r < 1 \tag{A16}$$

where b is another integration constant. Upon adding and subtracting, we find two pairs of dual integral equations for ψ and χ:

$$\int_0^\infty J_1(kr)\tilde{\psi}(k)\, dk \;=\; \frac{d}{2r} \qquad 1 < r \tag{A17}$$

$$\int_0^\infty J_1(kr)\tilde{\psi}(k)\, dk \;=\; -\frac{1}{4}(b+S)r \qquad 0 < r < 1 \tag{A18}$$

and

$$\int_0^\infty J_1(kr)\tilde{\chi}(k)\, dk \;=\; \frac{d}{2r} \qquad 1 < r \tag{A19}$$

$$\int_0^\infty J_1(kr)\tilde{\chi}(k)\, dk \;=\; \frac{1}{2}(b-S)r \qquad 0 < r < 1\,. \tag{A20}$$

Both these problems have the standard Titchmarsh form

$$\int_0^\infty J_1(kr)\tilde{c}(k)k\,dk \;=\; \frac{B}{r} \qquad 1 < r \tag{A21}$$

$$\int_0^\infty J_1(kr)\tilde{c}(k)\,dk \;=\; Ar \qquad 0 < r < 1 \tag{A22}$$

the solution of which is (see e.g. Sneddon [26] p.84)

$$\tilde{c} \;=\; \frac{2}{3}\sqrt{\frac{2}{\pi}}A\frac{J_{5/2}(k)}{\sqrt{k}} + B\frac{\sin k}{k}. \tag{A23}$$

With this result the Hankel transforms can be evaluated in their complementary intervals finding

$$\int_0^\infty J_1(kr)\tilde{c}(k)k\;dk = \left(B - \frac{4A}{3\pi}\right)\frac{1}{r\sqrt{r^2-1}} - \frac{4A}{2\pi r}\left[\sqrt{r^2-1} - r^2\text{arcsin}\left(\frac{1}{r}\right)\right] \qquad r > 1 \tag{A24}$$

$$\int_0^\infty J_1(kr)\tilde{c}(k)dk = \frac{4}{3}\frac{A}{\pi}r\sqrt{1-r^2} + B\frac{1-\sqrt{1-r^2}}{r} \qquad 0 < r < 1. \tag{A25}$$

The second expression is regular at $r = 0$ provided that

$$B = \frac{4A}{3\pi}. \tag{A26}$$

Upon imposing this condition on the solutions for ψ and χ we find

$$d \;=\; -\frac{8}{9\pi}S\,, \qquad b \;=\; \frac{1}{3}S \tag{A27}$$

so that, finally,

$$\tilde{\psi} \;=\; \tilde{\chi} \;=\; -\frac{4S}{3\sqrt{2\pi}}\frac{J_{3/2}(k)}{\sqrt{k}} \;=\; \frac{4S}{3\pi}\frac{k\cos k - \sin k}{k^3} \tag{A28}$$

The velocity field inside the disk is readily calculated from these expressions finding

$$v_x(r,0,\theta) \;=\; -\frac{4S}{3\pi}\sqrt{1-r^2} \qquad v_y(r,0,\theta) \;=\; 0. \tag{A29}$$

The average velocity over the disk is found from direct integration:

$$\frac{1}{\pi}\int_0^{2\pi} d\theta \int_0^1 rdr\; v_x(r,0,\theta) = -\frac{8S}{3\pi}\int_0^1 r\sqrt{1-r^2}dr \;=\; -\frac{8}{9\pi}S \tag{A30}$$

while the y component vanishes. Although not necessary for the solution of the problem at hand, it may be of interest to also show explicitly the expressions for the velocity and pressure fields away from the disk. With the definitions:

$$\ell_1 = \frac{1}{2}[\sqrt{(r+1)^2+z^2} - \sqrt{(r-1)^2+z^2}] \tag{A31}$$

$$\ell_2 = \frac{1}{2}[\sqrt{(r+1)^2+z^2} + \sqrt{(r-1)^2+z^2}] \tag{A32}$$

the integrals can be evaluated to find (see Gradshteyn & Ryzhik [9] sections 6.621, 6.751 and 6.752)

$$\begin{aligned} v_x(r,z,\theta) = -\frac{2Sz}{3\pi}r^2\frac{\sqrt{\ell_2^2-1}}{(\ell_2^2-\ell_1^2)\ell_2^4}\text{cos}2\theta - \frac{4S}{3\pi}\left(\sqrt{1-\ell_1^2} - z\text{arcsin}\left(\frac{1}{\ell_2}\right)\right) \\ -\frac{2Sz}{3\pi}\left(\frac{\sqrt{\ell_2^2-1}}{(\ell_2^2-\ell_1^2)} - \text{arcsin}\left(\frac{1}{\ell_2}\right)\right) \end{aligned} \tag{A33}$$

$$v_y(r,z,\theta) = -\frac{2Sz}{3\pi} r^2 \frac{\sqrt{\ell_2^2-1}}{(\ell_2^2-\ell_1^2)\ell_2^4} \sin 2\theta \tag{A34}$$

$$v_z(r,z,\theta) = \frac{4Sz}{3\pi}\left(-\frac{\ell_1^2\sqrt{1-\ell_1^2}}{(\ell_2^2-\ell_1^2)r}\right)\cos 2\theta \tag{A35}$$

$$p(r,z,\theta) = \frac{8S\mu}{3\pi}\left(-\frac{\ell_1^2\sqrt{1-\ell_1^2}}{(\ell_2^2-\ell_1^2)r}\right)\cos 2\theta \tag{A36}$$

APPENDIX B: SOLUTION OF THE TWO-DIMENSIONAL PROBLEM

In this case it is convenient to adopt as fundamental length $\frac{1}{2}a$ and a Cartesian system of coordinates with x along the plane direction and y along the normal. The Boundary conditions of the Stokes problem for v_x and v_y become

$$v_x(x,0) = 0 \qquad |x| > 1 \tag{B1}$$

$$\partial_y v_x(x,0) = S \qquad |x| < 1. \tag{B2}$$

$$v_y(x,0) = 0 \qquad -\infty < x < \infty\,. \tag{B3}$$

where

$$S = -\frac{1}{\mu}\langle \tau_{xy}\rangle. \tag{B4}$$

We introduce a stream function ψ in terms of which

$$v_x(x,y) = \partial_y \psi\,, \qquad v_y(x,y) = -\partial_x \psi \tag{B5}$$

and

$$\omega = \partial_y v_x - \partial_x v_y = \Delta\psi. \tag{B6}$$

The vorticity ω is harmonic and can be written as a Fourier integral in the form

$$\omega(x,y) = \int_{-\infty}^{\infty} dk \exp(ikx)\tilde{\omega}(k) e^{-|k|y}. \tag{B7}$$

By introducing the Fourier transform $\tilde{\psi}(k,y)$ of the stream function, substituting into (B6), and integrating, we find

$$\tilde{\psi}(k,y) = -\frac{y\tilde{\omega}(k)}{2|k|} e^{-|k|y} \tag{B8}$$

after elimination of an integration constant on the basis of (B3). With this result, the boundary condition (B1) becomes

$$\int_{-\infty}^{\infty} dk \exp(ikx)\tilde{\omega}(k) = S \qquad |x| < 1 \tag{B9}$$

and (B2)

$$\int_{-\infty}^{\infty} dk \exp(ikx)\frac{\omega\tilde{(k)}}{|k|} = 0 \qquad |x| > 1\,. \tag{B10}$$

Upon writing (B9) for x and -x and adding or subtracting, we find

$$\int_{-\infty}^{\infty} dk \cos(kx)\tilde{\omega}(k) = S \qquad 0 < x < 1 \tag{B11}$$

$$\int_{-\infty}^{\infty} dk \sin(kx)\tilde{\omega}(k) = 0 \qquad 0 < x < 1. \tag{B12}$$

Proceeding in a similar way with (B10) we have

$$\int_{-\infty}^{\infty} dk \cos(kx)\frac{\tilde{\omega}(k)}{|k|} = 0 \qquad 1 < x \tag{B13}$$

$$\int_{-\infty}^{\infty} dk \sin(kx)\frac{\tilde{\omega}(k)}{|k|} = 0 \qquad 1 < x. \tag{B14}$$

If in (B11) we separate the integration range into $-\infty < k < 0$ and $0 < k < \infty$ we find

$$\int_{0}^{\infty} dk \cos(kx)\tilde{\omega}_{+} = S \qquad 0 < x < 1 \qquad \tilde{\omega}_{+} \;=\; \tilde{\omega}(k) + \tilde{\omega}(-k) \tag{B15}$$

whereas (B12) gives

$$\int_{0}^{\infty} dk \sin(kx)\tilde{\omega}_{-} = 0 \qquad 0 < x < 1 \qquad \tilde{\omega}_{-} \;=\; \tilde{\omega}(k) - \tilde{\omega}(-k). \tag{B16}$$

Similarly

$$\int_{0}^{\infty} dk \cos(kx)\frac{\tilde{\omega}_{+}}{k} = 0 \qquad 1 < x \tag{B17}$$

$$\int_{0}^{\infty} dk \sin(kx)\frac{\tilde{\omega}_{-}}{k} = 0 \qquad 1 < x. \tag{B18}$$

Since the problem for $\tilde{\omega}_{-}$ is completely homogeneous, this quantity must vanish so that $\tilde{\omega}(k)$ is even in k and, therefore, real. We are thus led to the pair of dual integral equations

$$\int_{0}^{\infty} dk \cos(kx)\tilde{\omega} = \frac{1}{2}S \qquad 0 < x < 1 \tag{B19}$$

$$\int_{0}^{\infty} dk \cos(kx)\frac{\tilde{\omega}}{k} = 0 \qquad 1 < x. \tag{B20}$$

This is a standard problem with the solution (see e.g. Sneddon [26] p. 84)

$$\tilde{\omega}(k) \;=\; \frac{1}{2}SJ_1(k) \tag{B21}$$

from which the velocity on the boundary follows as

$$v_x(x,0) = -\frac{S}{2}\cos\left(\arcsin x\right) \;=\; -\frac{S}{2}\sqrt{1-x^2} \qquad x < 1 \tag{B22}$$

so that

$$\frac{1}{2}\int_{-1}^{1} v_x(x,0)dx = -\frac{\pi}{8}S. \tag{B23}$$

This result coincides with that derived by different means in Philip [17]. As before, it may be of some interest to show the explicit results for the velocity and pressure fields. One has

$$v_x(x,y) \;=\; -\frac{S}{2}\int_{-\infty}^{\infty} dk\,\cos(kx)\left(\frac{1}{|k|}-y\right)\tilde{\omega}(k)e^{-|k|y} \tag{B24}$$

$$v_y(x,y) \;=\; -\frac{S}{2}\int_{-\infty}^{\infty} dk\,\sin(kx)y\tilde{\omega}(k)e^{-|k|y} \tag{B25}$$

$$p(x,y) \;=\; -2S\int_{0}^{\infty} dk\,\sin(kx)\tilde{\omega}(k)\,e^{-ky}. \tag{B26}$$

The integrals can be evaluated to find

$$v_x(x,y) = -\frac{S}{2}R(x,y) - \frac{yS}{2}\partial_y R(x,y) \tag{B27}$$

$$v_y(x,y) = \frac{yS}{2}\partial_y I(x,y) \tag{B28}$$

$$p(x,y) = S\partial_y R(x,y) \tag{B29}$$

with

$$R(x,y) = -y + \sqrt{\frac{(1-x^2+y^2)+\sqrt{(1-x^2+y^2)^2+4x^2y^2}}{2}} \tag{B30}$$

$$I(x,y) = x + \sqrt{\frac{-(1-x^2+y^2)+\sqrt{(1-x^2+y^2)^4+4x^2y^2}}{2}}\,. \tag{B31}$$

---

[1] Barthlott, W. & Neinhaus, C., "Purity of the sacred lotus, or escape from contamination in biological surfaces"", *Planta* **202**, 1–8 (1997).
[2] Bunkin, N. F., Kochergin, A. V., Lobeyev, A. V., Ninham, B. W. & Vinogradova, O. I.,"Existence of charged submicrobubble clusters in polar liquids as revealed by correlation between optical cavitation and electrical conductivity", *Colloid Int. Sci.* **A110**, 207–212 (1996).
[3] Cheng, J.-T. & Giordano, N.," Fluid flow through nanometer-scale channels" *Phys. Rev. Lett.* **65**, 031206 (2002).
[4] Choi, C. H. & Kim, C. J., "Large slip of aqueous liquid flow over a nanoengineered superhydrophobic surface", *Phys. Rev. Lett.* **96**, 066001 (2006).
[5] Craig, V. S. J., Neto, C. & Williams, D. R. M., "Shear-dependent boundary slip in an aqueous Newtonian liquid" *Phys. Rev. Lett.* **87**, 054504 (2001).
[6] Dammer, S. M. & Lohse, D.," Gas enrichment at liquid-wall interfaces" *Phys. Rev. Lett.* **96**, 206101 (2006).
[7] Davis, A. M. J.,"Shear flow disturbance due to a hole in the plane" *Phys. Fluids* **A3**, 478–480 (1991).
[8] Foldy, L., "The multiple scattering of waves" *Phys. Rev.* **67**, 107–119 (1945).
[9] Gradshteyn, I. S. & Ryzhik, I. M., *Table of Integrals, Series, and Products*, 6th edn. San Diego: Academic Press (2000).
[10] Holmberg, M., Kühle, A., Garnaes, J., Mørch, K. A. & Boisen, A., "Nanobubble trouble on gold surfaces" *Langmuir* **19**, 10,510–10,513 (2003).
[11] Ishida, N., Inoue, T., Miyahara, M. & Higashitani, K.," Nano bubbles on a hydrophobic surface in water observed by tapping-mode atomic force microscopy" *Langmuir* **16**, 6377–6380 (2000).
[12] Kim, S. & Karrila, S., *Microhydrodynamics*. Boston: Butterworth-Heinemann (1991).

[13] Lauga, E., Brenner, M. P. & Stone, H. A., Microfluidics: the no-slip boundary condition. In *Handbook of Experimental Fluid Dynamics* (ed. J. Foss, C. Tropea & A. Yarin), to appear, New York: Springer (2005).
[14] Lauga, E. & Stone, H. A.,"Effective slip in pressure-driven stokes flow" *J. Fluid Mech.* **489**, 55–77 (2003).
[15] Ou, J., Perot, B. & Rothstein, P., "Laminar drag reduction in microchannels using ultrahydrophobic surfaces" *Phys. Fluids* **16**, 4635–4643 (2004).
[16] Ou, J. & Rothstein, P., "Direct velocity measurement of the flow past drag-reducing ultrahydrophobic surfaces" *Phys. Fluids* **17**, 103606 (2005).
[17] Philip, J. R.,"Flows satisfying mixed no-slip and no-shear conditions", *Z. Angew. Math. Phys.* **23**, 353–370 (1972).
[18] Pit, R., Hervet, H. & Léger, L., "Direct experimental evidence of slip in hexadecane: Solid interfaces" *Phys. Rev. Lett.* **85**, 980–983 (2000).
[19] Pozrikidis, C.,*Boundary Integral and Singularity Methods for Linearized Viscous Flow*. Cambridge: Cambridge U.P (1992).
[20] Ranger, K. B., "The circular disc straddling the interface of a two phase flow" *Int. J. Multiphase Flow* **4**, 263–277 (1978).
[21] Rubinstein, J. & Keller, J.," Sedimentation of a dilute suspension" *Phys. Fluids* **A1**, 637–643 (1989).
[22] Sarkar, K. & Prosperetti, A., "Effective boundary conditions for the Laplace equation with a rough boundary, *Proc. R. Soc. Lond.* **A451**, 425–452 (1995).
[23] Sarkar, K. & Prosperetti, A., "Effective boundary conditions for Stokes flow over a rough surface" *J. Fluid Mech.* **316**, 223–240 (1996).
[24] Simonsen, A. C., Hansen, P. L. & Klosgen, B.,"Nanobubbles give evidence of incomplete wetting at a hydrophobic interface" *J. Colloid Int. Sci.* **273**, 291–299 (2004).
[25] Smith, S. H.,"Stokes flows past slits and holes" *Int. J. Multiphase Flow* **13**, 219–231 (1987).
[26] Sneddon, I. N., *Mixed boundary value problems in potential theory*. Amsterdam: North-Holland (1966).
[27] Steitz, R., Gutberlet, T., Hauss, T., Klösgen, B., Krastev, R., Schemmel, S., Simonsen, A. C. & Findenegg, G. H.,"Nanobubbles and their precursor layer at the interface of water against a hydrophobic substrate" *Langmuir* **19**, 2409–2418 (2003).
[28] Tretheway, D. & Meinhart, C.,"Apparent fluid slip at hydrophobic microchannel walls" *Phys. Fluids* **14**, L9–L12 (2002).
[29] Twersky, V.,"On scattering and reflection of sound by rough surfaces" *J. Acoust. Soc. Am.* **29**, 209–225 (1957).
[30] Twersky, V.,"Reflection and scattering of sound by correlated rough surfaces" *J. Acoust. Soc. Am.* **73**, 85–94 (1983).
[31] Tyrrell, J. W. G. & Attard, P., "Images of nanobubbles on hydrophobic surfaces and their interactions" *Phys. Rev. Lett.* **87**, 176104 (2001).
[32] Vinogradova, O. I.,"Slippage of water over hydrophobic surfaces" *Int. J. Mineral Proc.* **56**, 31–60 (1999).
[33] Watanabe, K., Yanuar & Udagawa, H., "Drag reduction of Newtonian fluid in a circular pipe with a highly water-repellent wall" *J. Fluid Mech.* **381**, 225–238 (1999).
[34] Wu, Z., Zhang, X., Zhang, X., Li, G., Sun, J., Zhang, M. & Hu, J.," Nanobubbles influence on BSA adsorption on mica surface" *Surface Interface Anal.* **37**, 797–801 (2005).
[35] Zhu, Y. & Granick, S.," Rate-dependent slip of newtonian liquid at smooth surfaces" *Phys. Rev. Lett.* **87**, 096105 (2001).
[36] Zhu, Y. & Granick, S.," Limits of the hydrodynamic no-slip boundary condition" *Phys. Rev. Lett.* **88**, 106102 (2002).
[37] For the present purposes a curved boundary can be considered plane provided the radius of curvature is large compared with the size of the free-slip regions and their mean reciprocal distance, of order $a/\beta^{1/2}$.